

# Dynamics and correlations at a quantum phase transition beyond Kibble-Zurek

Krishanu Roychowdhury<sup>1</sup>, Roderich Moessner<sup>2</sup>, and Arnab Das<sup>3</sup>

<sup>1</sup>Department of Physics, Stockholm University, SE-106 91 Stockholm, Sweden

<sup>2</sup>Max Planck Institute for the Physics of Complex Systems, Nöthnitzer Straße 38, 01187 Dresden, Germany and

<sup>3</sup>Indian Association for the Cultivation of Science (School of Physical Sciences),  
2A & 2B Raja S. C. Mullick Road, Kolkata 700032, India

When a quantum phase transition is traversed by tuning a parameter of a Hamiltonian, Kibble-Zurek (KZ) theory stands out as the most robust theory of defect generation in such a process. We show how interesting nonequilibrium correlations can develop in the so-called impulse regime, which KZ treats as effectively static: in an integrable spin chain, domain wall (kink) correlators develop *Gaussian spatial decay*, while the spin correlators only fall off exponentially. We propose a simple but general framework beyond KZ, based on thermalization at an effective temperature in the impulse regime. Our dual description in terms of bosonic and fermionic degrees of freedom comprehensively accounts for the observed correlators, and leads us to a novel generalised Gibbs ensemble. We outline how to extend our picture to generic interacting situations.

*Introduction:* The Kibble-Zurek mechanism (KZM) provides arguably the simplest and most robust theory that captures the dynamics of a continuous quantum phase transition (QPT) both in the classical [1–5] and quantum [6–14] realms. Where a parameter (temperature/coupling) is ramped across the transition point at a finite rate, it predicts the universal scaling of the resulting defect density with the ramp rate (Kibble-Zurek (KZ) scaling laws). This relies on the so-called adiabatic-impulse (AI) approximation, which approximates the dynamics into two qualitatively different regimes. One is the adiabatic regime (away from the transition point), where the state evolves adiabatically with the change in the tuning parameter; the other is the impulse regime where the state of the system is considered to be effectively frozen as equilibration slows down near the critical point. The powerful simplicity of KZM continues to underpin an ever expanding field of complex dynamics of a QPT. Universal features of the scaling associated with KZM have been shown to emerge for various quench protocols and extend to observables besides the local defect density [15–17]. Remarkably, the mechanism seems to be more robust than its underlying key approximation (i.e., the AI approximation) in predicting defect densities [18]: the dynamics in the impulse regime merely renormalizes the prefactors, leaving the scaling laws intact.

Here we explore correlations and dynamics of traversing a QPT beyond the KZ framework. Instead of merely the density of defects, we focus on *correlations* between them, specifically in the impulse regime about which the AI picture by its starting assumption has little to say. We show that for a slow ramp, these defect correlations can acquire surprising forms during the ramp which persist to the later stage of the dynamics. We show that a simple yet general theory extends the KZ picture; it emerges from the complexity of the dynamics and invokes thermalization at an effective nonzero temperature.

For a concrete demonstration, we consider the fruitfly of QPT [19], namely, an integrable Ising chain in a transverse field, and ramp it linearly through a critical point. We study the spatial correlators between kinks, which show *Gaussian spatial decay*, while the spin correlators show the usual exponential behavior. Our theory accounts for this unusual

Gaussian spatial decay, and also provides the physical basis for long-known oscillatory correlations [20]. We then demonstrate that the simplicity of our theory stems from the complex nonequilibrium dynamics of the slow ramp, and cannot be extracted from the behavior of any eigenstates (including the ground state) of the Hamiltonian for any value of the parameter within the ramp range. We also consider the stability of the correlations at long times after the ramp is stopped: we show that the Gaussian correlations survive to infinitely late times. This identifies a novel generalized Gibbs' Ensemble (GGE). Last but not the least, we show our results do not contradict KZ, but focus on aspects of the dynamics of QPT which does not fall within its remit, and we show how our picture connects with KZ; in particular, length and time-scales appearing in the novel defect correlations exhibit KZ scaling.

*Model and Protocol:* Our transverse field Ising chain [19, 21]

$$\mathcal{H}(g) = -\frac{J}{2} \sum_{j=1}^N (\sigma_j^x \sigma_{j+1}^x + g \sigma_j^z), \quad (1)$$

is periodic  $\sigma_{N+1}^x = \sigma_1^x$  and has even number of spins  $N$ . We set the overall energy scale  $J = 1$ , so that  $g$  is the dimensionless transverse field strength. It is ramped from  $+\infty$  to 0 over time  $\tau_Q$ ,  $g(t) = -t/\tau_Q$ , crossing a critical point at  $g_c = 1$  between paramagnet for  $|g| > 1$ , and ferromagnet otherwise.

The following transformation [22] to dual variables  $\mu^{x,z}$  is particularly useful for calculating the correlators of interest:

$$\mu_j^z = \sigma_j^x \sigma_{j+1}^x ; \quad \mu_j^x = \prod_{k < j} \sigma_k^z, \quad (2)$$

$$\tilde{\mathcal{H}} = -\frac{1}{2} \sum_j (g \mu_j^x \mu_{j+1}^x + \mu_j^z).$$

Fermionization [23, 24] of  $\tilde{\mathcal{H}}$ :  $\mu_j^x = (c_j^\dagger + c_j) \prod_{l < j} (1 - 2c_l^\dagger c_l)$ ;  $\mu_j^z = 1 - 2c_j^\dagger c_j$ , reduces this to an ensemble of two level systems in momentum space [9] after Fourier transformation of the fermion operator  $c_j = (1/\sqrt{N}) \sum_k e^{ikj} c_k$  (ap-

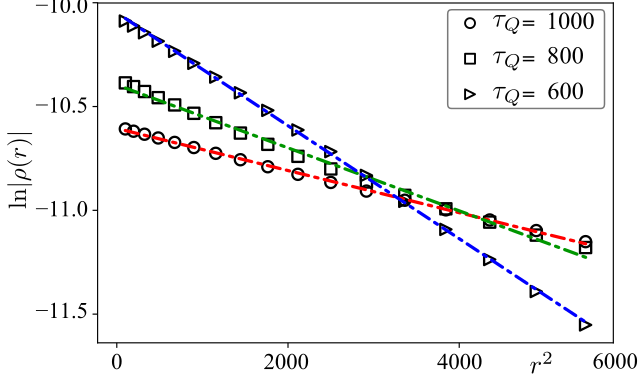


FIG. 1. **Gaussian decay of the kink correlator:** numerical results (for  $N = 10^4$ ) right after the ramp ending at  $g = 0$  (empty symbols). The dashed lines are their corresponding Gaussian fits.

appropriate boundary conditions suitable for the even fermion-parity sector fix the allowed values of  $k$  [25]).

The time-dependent ground state wavefunction, which is a tensor product  $|\Psi_G(t)\rangle \equiv \otimes_k |\Psi_k(t)\rangle$ , is obtained following a time-dependent Bogoliubov-de Gennes (TDBdG) transformation:  $c_k(t) = u_k(t)\gamma_k + v_{-k}^*(t)\gamma_{-k}^\dagger$ , and demanding the state to be annihilated by the Bogoliubov fermions ( $\gamma_k$ ) at every instant of the evolution:  $\gamma_k|\Psi_k(t)\rangle = 0$ . Note we have assumed the Heisenberg picture where the operators' equations of motion are  $i\frac{d}{dt}c_k = [c_k, \mathcal{H}]$  with  $\frac{d}{dt}\gamma_k = 0$  [9]. The coefficients  $u_k(t)$  and  $v_k(t)$  of  $|\Psi_k(t)\rangle \equiv [u_k(t) v_k(t)]^T$  satisfy

$$i\frac{d}{dt}|\Psi_k(t)\rangle = [\tau_k^z(1 - g \cos k) + \tau_k^y g \sin k]|\Psi_k(t)\rangle, \quad (3)$$

where  $\tau_k^{y,z}$  are Pauli matrices defined for each  $k$ . Initially prepared in the ground state  $|\Psi_i\rangle \equiv \otimes_k |\Psi_k(t \rightarrow -\infty)\rangle = \otimes_k [1 \ 0]^T$ , the system's observables at the end of the ramp are calculated via  $u_k(t)$  and  $v_k(t)$  obtained by solving Eq. 3.

*Asymptotic Solution and Kink Correlator:* The TDBdG can be brought to the standard form via  $|\Psi_k\rangle \rightarrow |\tilde{\Psi}_k\rangle = U_k|\Psi_k\rangle$  with  $U = \text{Exp}[-i(k/2)\tau^y]\text{Exp}[i(\pi/4)(\tau^z - 1)]$  leading to the Landau-Zener-Stückelberg type problem  $d|\tilde{\Psi}_k\rangle/d\tau = -i(\tau^z\epsilon + \tau^x\Delta)|\tilde{\Psi}_k\rangle$ , where  $|\tilde{\Psi}_k\rangle \equiv [\tilde{u}_k \ \tilde{v}_k]^T$  and  $\tau = t + \tau_Q \cos k$ ,  $\epsilon = \tau/\tau_Q$ ,  $\Delta = \sin k$ . The solutions are expressed in terms of parabolic cylinder functions [26] with the following asymptotics [27] for slow ramps,  $\tau_Q \gg 1$ .

At the end of the ramp ( $t = 0$ ),  $\tilde{u}_k = r_k e^{i\omega_k}$  and  $\tilde{v}_k = \text{sgn}(\Delta)\sqrt{1 - r_k^2}e^{i\phi_k}$  with  $r_k = e^{-\pi\tau_Q\Delta^2/2}$ ,  $\omega_k = \frac{3\pi}{4} - \frac{\tau^2}{2\tau_Q} - \frac{\tau_Q\Delta^2}{2}\ln\left(\tau\sqrt{2/\tau_Q}\right)$ , and  $\phi_k = \frac{\tau^2}{2\tau_Q} + \frac{\tau_Q\Delta^2}{2}\ln\left(\tau\sqrt{2/\tau_Q}\right) - \arg(\Gamma[1 + i\tau_Q\Delta^2/2])$ .  $u_k, v_k$  follow from  $|\Psi_k\rangle = U^\dagger|\tilde{\Psi}_k\rangle$ . Using these expressions, a simple analytic form of the correlation function can be achieved as the terms with the rapidly oscillating phases  $e^{i\omega_k}$  and  $e^{i\phi_k}$  can be ignored for  $\tau_Q \gg 1$  [27].

The correlators of primary concern are those between kinks

in the ferromagnetic phase (of the original model, Eq. 1) and generated in the course of the ramp in the vicinity of the critical point. The kinks are topological defects deep in the ferromagnetic phase where the ramp ends (at  $t = 0$ ) with their number scaling with the ramp time  $\tau_Q$  as  $n_d \sim \tau_Q^{-1/2}$  [7, 9].

Our first central result is this: the kink correlators feature an unusual *Gaussian* decay instead of more familiar exponential or power-law behavior. The spatial correlator in the longitudinal direction is of the form  $\hat{\rho}(r) = (1 - \sigma_j^x \sigma_{j+1}^x)(1 - \sigma_{j+r}^x \sigma_{j+r+1}^x)$  and the corresponding connected correlator is

$$\rho(r) = \langle \hat{\rho}(r) \rangle - \langle 1 - \sigma_j^x \sigma_{j+1}^x \rangle^2 = \langle \mu_j^z \mu_{j+r}^z \rangle - \langle \mu_j^z \rangle^2, \quad (4)$$

where the duality relations in Eq. 2 are invoked along with translation invariance. The expectation is with respect to the (time-independent) ground state of the Bogoliubov fermions. A straightforward calculation [27] gives in the limit  $N \rightarrow \infty$

$$\rho(r) \approx -\frac{1}{4\pi^2\tau_Q}e^{-r^2/2\pi\tau_Q} \quad (5)$$

for  $r \gg 1$ , verified numerically in Fig. 1. Such Gaussian form of the kink correlator is observed also for a full ramp from  $g = +\infty$  to  $g = -\infty$  [27]; as well as in the *transverse* correlator  $(1 - \sigma_j^z \sigma_{j+1}^z)(1 - \sigma_{j+r}^z \sigma_{j+r+1}^z)$  both for half and full ramps [27].

*Theory of the Defect Correlations:* Gaussian decay of correlations is not common in isolated many-body quantum systems. However, it is observed in dilute bosonic systems in low dimensions, including trapped ideal (see, e.g. [28–30]) or repulsive Bose gases [31]. In a Bose gas, the pair correlations are Gaussian at high temperature ( $T \gg T_{\text{QD}}$ ,  $T_{\text{QD}}$  denoting the temperature of quantum degeneracy) crossing over to exponential in the quantum limit ( $T \ll T_{\text{QD}}$ ). Our key observation here is that the kinks, likewise, are bosonic excitations. In the slow ramp limit ( $\tau_Q \gg 1$ ), the final state hosts *very dilute* kinks, which essentially behave as a thermally nondegenerate (classical) Bose gas.

Our simple thermal picture also naturally accounts for the long-known oscillatory behavior of the spin correlations at the end of a ramp across the QPT in an Ising chain [20]. Unlike the bosonic kink correlators, the spin correlators  $\langle \sigma_i^x \sigma_{i+r}^x \rangle$ , involve *fermions* [21]. Their two-point correlators  $\langle c_i^\dagger c_{i+r} \rangle$  and related observables are influenced by the formation of algebraic kink-antikink features on a length-scale set by the Fermi wavelength, with an exponential envelope due to the finite temperature. These oscillations are prominent at large ramp times (i.e. slow ramps), but vanish abruptly below a threshold value,  $\tau_Q^*$  [20]. For the fermionic modes, this corresponds to a thermal occupancy with  $T^* = 1/(4\pi\tau_Q^*)$  and dispersion  $\epsilon_k = \tau_Q^*/\tau_Q - \sin^2 k \leq 0$ . The pair of Fermi points present for  $\tau_Q > \tau_Q^*$  merge at zero wavevector when  $\tau_Q = \tau_Q^*$ , yielding a gap for  $\tau_Q < \tau_Q^*$  and terminating the oscillatory behavior [27].

Our theory should be robust even in generic systems, i.e. in presence of (weak) interactions: neither of its two

necessary elements – small density of defects at slow ramps, and an effective thermal environment – relies on the absence of interaction/integrability. In fact, a thermal local environment is to be expected from the eigenstate thermalization hypothesis (ETH) [32–36] in an interacting system driven out of equilibrium. Moreover, a small residual interaction between the bosonic excitations does not affect the Gaussian behavior at large separations, but only modifies it at small distances with corrections of the form  $\delta\rho(r) = -(2\gamma/nr)(T/T_{\text{QD}})^{-1} \text{Exp}[-(n^2r^2/2)(T/T_{\text{QD}})]$  where  $\gamma$  and  $n$  correspond to the interaction strength and boson density respectively [31]. This also exhibits Gaussian behavior at large  $r$ .

*Absence of Gaussian Correlations in Eigenstates:* Here, we demonstrate that our simple picture emerges from the complex dynamics of slow ramps, and cannot be derived simply from the knowledge of the equilibrium (eigenstates of the static Hamiltonian for the entire parameter range of the ramp), or as a result of an instantaneous quench. Recall that KZ assumes that the system remains in its ground state until at  $t = +\hat{t}$ , where it falls out of equilibrium and effectively stops evolving. This way, the properties of the equilibrium state (i.e., the ground state) in one phase is used for obtaining excitations in the other phase. It is, hence, imperative to ask whether the Gaussian decay after the ramp is likewise inherited from the ground state of the Hamiltonian  $\mathcal{H}(g)$  (Eq. 1) for some parameter value in the initial phase.

The answer is no: the ground state correlations decay exponentially for any  $|g| \neq g_c$ . In detail, in the ground state of  $\mathcal{H}(g)$ ,  $\rho(r) = -G(r)G(-r)$  where  $G(r) = (1/\pi) \int_0^\pi dk \mathcal{G}$  with  $\mathcal{G} = [\cos(kr) - g \cos(kr - k)]/\sqrt{1 - 2g \cos k + g^2}$ .  $G(r)$  involves regularized hypergeometric functions whose asymptotes at large values of  $r$  yield the falling exponential  $e^{-r/\xi_0}$  with the correlation length  $\xi_0$  diverging at  $g = g_c$  [27]. In fact our investigation suggests that the non-Gaussian behavior is generic also to excited eigenstates of all sorts of energy densities. One family of such (excited) eigenstates can be prepared by altering the occupation of all  $k$ -modes up to a certain value  $k^* \in [0, \pi]$  [37] ( $k^* = 0$  implying the ground state and  $k^* = \pi$  implying the highest excited state) corresponding to an energy density  $\bar{E} = (2/\pi) \int_0^{k^*} dk \sqrt{1 - 2g \cos k + g^2}$ .  $G(r)$ , in this case, takes the form  $G(r) = (1/\pi) \int_0^\pi dk \text{sgn}(k - k^*)\mathcal{G}$ . Any excited state prepared by occupying a randomly selected set of  $k$ -modes in  $[0, \pi]$  with a given probability density function would also contain the same algebraic factors as in  $\mathcal{G}$ , and so, the resultant correlation function cannot display any Gaussian—unless a Gaussian factor is explicitly present already in  $\mathcal{G}$  which, of course, is the case for the ramp owing to the functional forms of  $u_k$  and  $v_k$  noted previously [27]. This eliminates possible AI type explanations of the Gaussian spatial decay, as the evolution of the wavefunction away from the ground states needs to be taken into account.

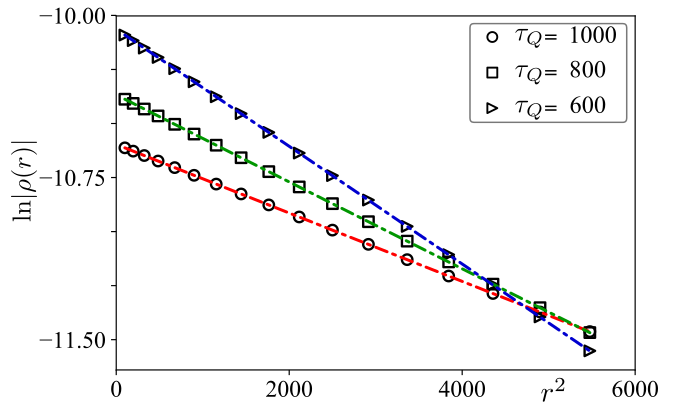


FIG. 2. **Kink correlations at long times:** numerical results at long times after the ramp is stopped at  $g = 0$  showing persistent Gaussian decay (empty symbols) at different values of  $\tau_Q$ . The same correlation function calculated from the GGE is shown in dashed lines (data shown for  $N = 10^4$ ).

*Late Time Correlations After the Ramp and resulting GGE:*

The Gaussian behavior is observed to persist in the long-time limit after the ramp is stopped and the system is allowed to evolve with a time-independent final Hamiltonian frozen at  $g = 0$  [Fig. 2] [27]. This amounts to a GGE with the density matrix  $\rho_{\text{GGE}} = Z^{-1} e^{-\sum_k \lambda_k J_k}$  ( $Z = \text{Tr}[e^{-\sum_k \lambda_k J_k}]$ ) and  $\lambda_k = \ln[(1 - \langle \psi_0 | J_k | \psi_0 \rangle) / \langle \psi_0 | J_k | \psi_0 \rangle]$ . Here the information of the “initial state” (reached at the end of the ramp) is encoded in the Lagrange multipliers  $\lambda_k$  corresponding to the conserved quantities  $J_k = \gamma_k^\dagger \gamma_k$  [38]. The Gaussian decay is inherited from the state produced by the ramp and imprinted in the Lagrange multipliers [for details, see 27]. Such a feature is absent in a GGE that arises due to an instantaneous quench from a simple initial state under a time-independent Hamiltonian [e.g. the ground state or any eigenstate of  $\mathcal{H}(g)$ ] as none of its eigenstates display Gaussian correlations for the defects.

A high density of defects produced in an instantaneous quench implies strong interactions among the defects, which can then obliterate the Gaussian correlations; conversely the state prepared in a slow ramp produces defects far apart, where Gaussian correlations may be present for sufficiently weak interactions, by analogy to the dilute Bose gas discussed above. It will be interesting to study the cross-over between these regimes in more detail.

*Relation to KZ:* While the form of the correlations are beyond the KZ framework, it nonetheless accounts for the scaling of most of the relevant length and time scales, reflecting the critical slowing down as a central ingredient [39].

We begin with Eq. 5, where it is the scale of the Gaussian decay:  $\xi \sim \tau_Q^{1/2}$  which reflects KZ scaling [9]. Also, Gaussian behavior sets in at  $g(t) = g^*$  which in turn obeys KZ scaling:  $\hat{g} = (g^* - g_c)/g_c \sim \tau_Q^{-1/2}$ . As a heuristic

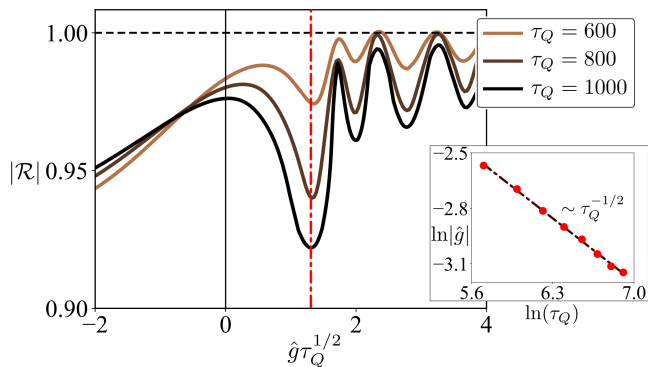


FIG. 3. **KZ scaling of the set-in time for the Gaussian decay:** (a) Pearson correlation coefficient  $|\mathcal{R}|$  versus KZ-scaled  $\hat{g}$  (defined in the text) revealing the extrema coincide (the primary one guided by the red dashed line) when  $\hat{g} \rightarrow \hat{g}\tau_Q^{1/2}$ . **Inset:** Set-in time  $\hat{g}$  of the Gaussian behavior against  $\tau_Q$  confirming KZ scaling  $\hat{g} \sim \tau_Q^{-1/2}$  (data shown for  $N = 10^4$ ).

for determining the set-in point  $\hat{g}$ , we consider estimating the (absolute value of the) Pearson correlation coefficient ( $|\mathcal{R}| \in [0, 1]$ ) for the plot of  $\ln|\rho(r)|$  against  $r^2$  [for details, see 27] as a function of  $\hat{g}$  for different values of  $\tau_Q$ . For a perfectly linearly correlated dataset ( $X = \{x_i\}, Y = \{y_i\}$ ),  $|\mathcal{R}|$  is 1. Accordingly, if the dataset is perfectly Gaussian correlated,  $|\mathcal{R}|$  is 1 for  $X = \{x_i^2\}$  and  $Y = \{\ln|y_i|\}$ . Following this, we compute  $|\mathcal{R}|$  for the dataset  $\mathcal{D} := \{(r_i^2, \ln|\rho_i|)\}$  and mark the location of the first minimum (from the critical point  $g_c = 1$ ) which reveals KZ scaling of  $\hat{g}$ :  $\hat{g} \sim \tau_Q^{-1/2}$  (Fig. 3 inset). For illustration, in Fig. 3 main, we plot the behavior of  $\mathcal{R}$  against the KZ-scaled  $\hat{g}$  such that the extrema for different values of  $\tau_Q$  coincide.

*Near-time Experimental Realm:* The novel correlations should be accessible experimentally using programmable Rydberg atomic quantum simulators [40] or Ising model simulators using superconducting qubits [41]. KZM has already been simulated using both setups. We thus require knowledge of the correlations for parameter values corresponding to currently accessible system sizes and timescales. In Fig. 4, we show the characteristic behavior for parameter ranges well below the analytical requirement  $\tau_Q \gg 1$ . For comparison, the regime accessed by experiments is  $\tau_Q \approx 14$  for a many-body Rydberg atom system [40] and  $\tau_Q \approx 620$  for a superconducting qubit simulator [41]. Note that, for  $\tau_Q = 5$ , the value of the short-distance correlations, due to the increased initial defect density, is considerably enhanced (Fig. 4), and thence the correlation decay quite accessible at short distances [for details of the spin correlation for rapid ramps, see 27].

*Summary:* We have provided an analysis of dynamics and

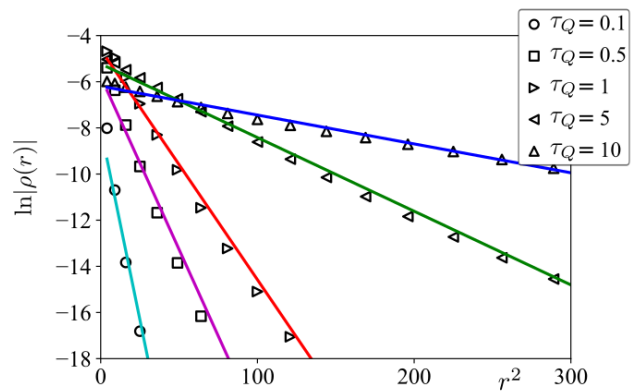


FIG. 4. **Gaussian decay of kink correlation for rapid ramps in small systems:** empty symbols are numerical results and the dashed lines are their corresponding Gaussian fits (data shown for  $N = 50$ ).

correlations beyond the AI scenario of KZ, effectively supplementing the ‘inert’ impulse regime with a thermalising dynamics of its own, following from the provision of a nontrivial initial state generated by the ramp. Our simple theory thus combines ideas from KZ with those from equilibration and quantum quenches; this has also led us to a novel type of GGE apparently naturally accessible only via such a route. Our picture is also attractive as the coexisting underlying fermionic/bosonic nature of different observables is crisply manifest in their qualitatively distinct (and unusual) correlations. There would appear to be considerable scope for theoretical studies to flesh out and extend this picture, as well as for testing it in experiment.

*Acknowledgements:* K.R acknowledges sponsorship, in part, by the Swedish Research Council. K.R and A.D acknowledge the Visitors Program of MPI-PKS for hospitality during a visit during which a part of the project was carried out. A.D acknowledges the partner group program Spin liquids: correlations, dynamics and disorder between IACS and MPI-PKS. This work was in part supported by the Deutsche Forschungsgemeinschaft under grants SFB 1143 (project-id 247310070) and the cluster of excellence ct.qmat (EXC 2147, project-id 39085490). The authors thank B. Doyon for a useful discussion, B. Damski for critical reading of the manuscript and many useful suggestions, and W. H. Zurek for very encouraging comments on the manuscript.

- 
- [1] T. W. B. Kibble, J. Phys. A **9**, 1378 (1976).
  - [2] T. W. B. Kibble, Phys. Rep. **67**, 183 (1980).
  - [3] W. H. Zurek, Nature **317**, 505 (1985).
  - [4] W. H. Zurek, Acta Phys. Pol. B **24**, 1301 (1993).
  - [5] W. H. Zurek, Phys. Rep. **276**, 177 (1996).
  - [6] B. Damski, Phys. Rev. Lett. **95**, 035701 (2005).
  - [7] W. H. Zurek, U. Dorner, and P. Zoller, Phys. Rev. Lett. **95**,



- 105701 (2005).
- [8] A. Polkovnikov, *Phys. Rev. B* **72**, 161201 (2005).
- [9] J. Dziarmaga, *Phys. Rev. Lett.* **95**, 245701 (2005).
- [10] V. Mukherjee, U. Divakaran, A. Dutta, and D. Sen, *Phys. Rev. B* **76**, 174303 (2007).
- [11] D. Sen, K. Sengupta, and S. Mondal, *Phys. Rev. Lett.* **101**, 016806 (2008).
- [12] J. Dziarmaga, *Advances in Physics* **59**, 1063 (2010).
- [13] A. Polkovnikov, K. Sengupta, A. Silva, and M. Vengalattore, *Rev. Mod. Phys.* **83**, 863 (2011).
- [14] L. Cincio, J. Dziarmaga, J. Meisner, and M. M. Rams, *Physical Review B* **79**, 094421 (2009).
- [15] A. Chandran, A. Erez, S. S. Gubser, and S. L. Sondhi, *Phys. Rev. B* **86**, 064304 (2012).
- [16] A. del Campo, *Phys. Rev. Lett.* **121**, 200601 (2018).
- [17] A. Chandran, F. Burnell, V. Khemani, and S. L. Sondhi, *Journal of Physics: Condensed Matter* **25**, 404214 (2013).
- [18] A. Francuz, J. Dziarmaga, B. Gardas, and W. H. Zurek, *Phys. Rev. B* **93**, 075134 (2016).
- [19] S. Sachdev, *Quantum Phase Transitions* (Cambridge University Press, 2011).
- [20] R. W. Cherng and L. S. Levitov, *Phys. Rev. A* **73**, 043614 (2006).
- [21] S. Suzuki, J.-i. Inoue, and B. K. Chakrabarti, *Quantum Ising phases and transitions in transverse Ising models*, Vol. 862 (Springer, 2012).
- [22] J. B. Kogut, *Rev. Mod. Phys.* **51**, 659 (1979).
- [23] E. Lieb, T. Schultz, and D. Mattis, *Annals of Physics* **16**, 407 (1961).
- [24] P. Jordan and E. P. Wigner, *Z. Phys.* **47**, 631 (1928).
- [25] B. Damski and M. M. Rams, *Journal of Physics A: Mathematical and Theoretical* **47**, 025303 (2013).
- [26] E. T. Whittaker and G. N. Watson, *A Course in Modern Analysis (4th Ed.)* (Cambridge University Press, 1990).
- [27] See Supplemental Material at [URL to be inserted by publisher] for details of the computation of parabolic cylinder functions and their asymptotes, calculations of the longitudinal and transverse kink correlators including the results for fast ramps from  $g = \infty \rightarrow 0$  and  $g = \infty \rightarrow -\infty$ , computation of the kink correlator in the static model, and construction of the GGE.
- [28] Z. Hadzibabic and J. Dalibard, *Rivista del Nuovo Cimento* **34**, 389 (2011).
- [29] M. Naraschewski and R. J. Glauber, *Phys. Rev. A* **59**, 4595 (1999).
- [30] T. M. Wright, A. Perrin, A. Bray, J. Schmiedmayer, and K. V. Kheruntsyan, *Phys. Rev. A* **86**, 023618 (2012).
- [31] A. G. Sykes, D. M. Gangardt, M. J. Davis, K. Viering, M. G. Raizen, and K. V. Kheruntsyan, *Phys. Rev. Lett.* **100**, 160406 (2008).
- [32] E. T. Jaynes, *Phys. Rev.* **106**, 620 (1957).
- [33] M. Srednicki, *Phys. Rev. E* **50**, 888 (1994).
- [34] M. Rigol, V. Dunjko, V. Yurovsky, and M. Olshanii, *Physical review letters* **98**, 050405 (2007).
- [35] A. C. Cassidy, C. W. Clark, and M. Rigol, *Physical review letters* **106**, 140405 (2011).
- [36] M. Rigol, V. Dunjko, and M. Olshanii, *Nature* **452**, 854 (2016).
- [37] S. Nandy, A. Sen, A. Das, and A. Dhar, *Phys. Rev. B* **94**, 245131 (2016).
- [38] L. Vidmar and M. Rigol, *Journal of Statistical Mechanics: Theory and Experiment* **2016**, 064007 (2016).
- [39] A. Das, J. Sabbatini, and W. H. Zurek, *Scientific Reports* **2**, 352 (2012).
- [40] A. Keesling, A. Omran, H. Levine, H. Bernien, H. Pichler, S. Choi, R. Samajdar, S. Schwartz, P. Silvi, S. Sachdev, P. Zoller, M. Endres, M. Greiner, V. Vuletić, and M. D. Lukin, *Nature* **568**, 207 (2019).
- [41] M. Gong, X. Wen, G. Sun, D.-W. Zhang, D. Lan, Y. Zhou, Y. Fan, Y. Liu, X. Tan, H. Yu, Y. Yu, S.-L. Zhu, S. Han, and P. Wu, *Scientific Reports* **6**, 22667 (2016).

# Supplemental material for “Dynamics at a quantum phase transition beyond Kibble-Zurek”

Krishanu Roychowdhury,<sup>1</sup> Roderich Moessner,<sup>2</sup> and Arnab Das<sup>3</sup>

<sup>1</sup>Department of Physics, Stockholm University, SE-106 91 Stockholm, Sweden

<sup>2</sup>Max Planck Institute for the Physics of Complex Systems, Nöthnitzer Straße 38, 01187 Dresden, Germany

<sup>3</sup>Indian Association for the Cultivation of Science (School of Physical Sciences),  
2A & 2B Raja S. C. Mullick Road, Kolkata 700032, India

## ASYMPTOTIC SOLUTION OF THE TDBdG EQUATION

We start with the Landau-Zener-Stückelberg type of differential equations (noted in the main text)

$$i \frac{d\tilde{u}_k(\tau)}{d\tau} = \frac{\tau}{\tau_Q} \tilde{u}_k(\tau) + \sin(k) \tilde{v}_k(\tau), \quad (1a)$$

$$i \frac{d\tilde{v}_k(\tau)}{d\tau} = -\frac{\tau}{\tau_Q} \tilde{v}_k(\tau) + \sin(k) \tilde{u}_k(\tau), \quad (1b)$$

which can be decoupled to yield

$$\left[ \frac{d^2}{d\tau^2} + \frac{i}{\tau_Q} + \frac{\tau^2}{\tau_Q^2} + \sin^2 k \right] \tilde{u}_k(\tau) = 0, \quad (2a)$$

$$\left[ \frac{d^2}{d\tau^2} - \frac{i}{\tau_Q} + \frac{\tau^2}{\tau_Q^2} + \sin^2 k \right] \tilde{v}_k(\tau) = 0. \quad (2b)$$

Introducing the variable  $z = \tau \sqrt{2/\tau_Q} e^{-i\pi/4}$ ,

$$\frac{d^2}{dz^2} \tilde{u}_k + \left[ n - \frac{1}{2} - \frac{z^2}{4} \right] \tilde{u}_k(z) = 0, \quad (3a)$$

$$\frac{d^2}{dz^2} \tilde{v}_k + \left[ n + \frac{1}{2} - \frac{z^2}{4} \right] \tilde{v}_k(z) = 0, \quad (3b)$$

where  $n = i(\tau_Q/2) \sin^2 k$ . It can be shown that if  $P(z)$  is a solution of Eq. 3b, then  $[z/2 + d/dz]P(z)$  is a solution of Eq. 3a. Eq. 3b represents the Weber equation whose solution is given in terms of complex parabolic cylinder functions  $\mathcal{D}_m(z)$  [1]

$$\tilde{v}_k(z) = A\mathcal{D}_{-n-1}(iz) + B\mathcal{D}_{-n-1}(-iz), \quad (4a)$$

$$\tilde{u}_k(z) = \frac{e^{i\pi/4}}{\sin k \sqrt{\tau_Q/2}} \left[ \frac{z}{2} + \frac{d}{dz} \right] \tilde{v}_k(z), \quad (4b)$$

where  $A, B$  are constants to be fixed by the initial conditions at  $\tau \rightarrow -\infty$ . The asymptotes of  $\mathcal{D}_m(z)$  are given by

$$\begin{aligned} \mathcal{D}_m(z) &\sim e^{-z^2/4} z^m [1 + \mathcal{O}(1/z^2)], & \forall -\frac{3\pi}{4} < \text{Arg}(z) < -\frac{\pi}{4}, \\ \mathcal{D}_m(z) &\sim \left( e^{-z^2/4} z^m - \frac{\sqrt{2\pi}}{\Gamma(-m)} e^{-im\pi} e^{z^2/4} z^{-(m+1)} \right) [1 + \mathcal{O}(1/z^2)]. & \forall -\frac{5\pi}{4} < \text{Arg}(z) < -\frac{\pi}{4}. \end{aligned} \quad (5)$$

Plugging the initial conditions  $\tilde{u}_k(\tau \rightarrow -\infty) = 1$  and  $\tilde{v}_k(\tau \rightarrow -\infty) = 0$ , we obtain

$$A = 0 ; B = \sin k \sqrt{\frac{\tau_Q}{2}} e^{-\pi\tau_Q \sin^2 k/8}. \quad (6)$$

Finally, we use the above asymptotes for  $\tau \rightarrow \infty$ , which for the ramps ending at  $g = 0$  is ensured by  $\tau_Q \gg 1$  (i.e. slow ramps) and for the ramps extended to  $g = -\infty$ , by  $g$  itself. We are then lead to the expressions of  $\tilde{u}_k, \tilde{v}_k$  noted in the main text.

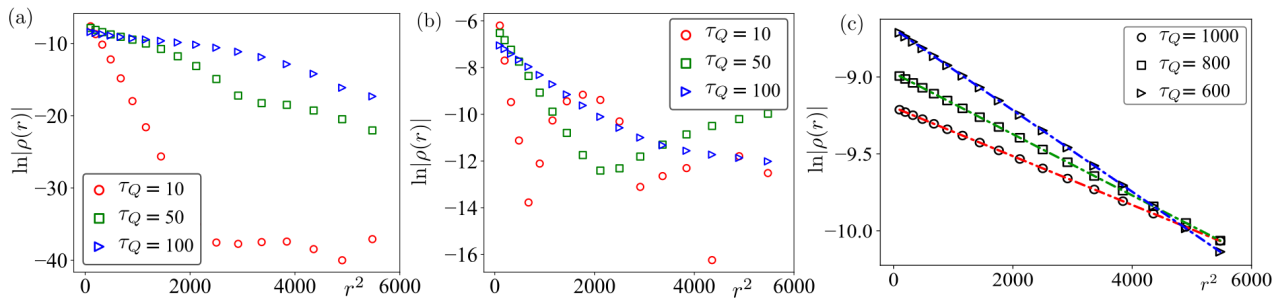


FIG. 1. Nonequilibrium results right after the ramp ending at  $g = 0$  in (a) and  $g = -\infty$  in (b) [data shown for  $N = 10^4$ ] for faster ramps showing deviation from Gaussian compared to the ones presented in Fig. 1 of the main text. (c) Results for the ramp ending at  $g = -\infty$  for large values of  $\tau_Q$ . Empty symbols represent the data, and the lines the corresponding Gaussian fit.

### COMPUTATION OF THE KINK CORRELATION FUNCTION IN THE LONGITUDINAL DIRECTION

As noted in the main text, the kink correlation function in the longitudinal direction, in terms of the dual variables, is

$$\rho(r) = \langle \mu_j^z \mu_{j+r}^z \rangle - \langle \mu_j^z \rangle^2, \quad (7)$$

which, following the substitution  $\mu_j^z = 1 - 2c_j^\dagger c_j$ , reads

$$\begin{aligned} \rho(r) &= 4\langle c_j^\dagger c_j c_{j+r}^\dagger c_{j+r} \rangle - 4\langle c_j^\dagger c_j \rangle^2 \\ &= \frac{4}{N^2} \left[ \sum_{k>0} |v_k|^2 e^{-ikr} \sum_{l>0} |u_l|^2 e^{-ilr} - \left| \sum_{k>0} u_k v_k^* e^{-ikr} \right|^2 \right], \end{aligned} \quad (8)$$

where we have exploited the relation that diagonalizes the dual Hamiltonian  $\tilde{\mathcal{H}}$ , viz.,

$$c_j = \frac{1}{\sqrt{N}} \sum_k e^{ikj} (u_k \gamma_k + v_{-k}^* \gamma_{-k}^\dagger), \quad (9)$$

noting the fact that the state with respect to which the above correlation is measured is a Bogoliubov vacuum. We obtain the expressions of  $u_k, v_k$  as

$$u_k = \cos(k/2) \tilde{u}_k + \sin(k/2) \tilde{v}_k; \quad v_k = -i \sin(k/2) \tilde{u}_k + i \cos(k/2) \tilde{v}_k, \quad (10)$$

where the expressions of  $\tilde{u}_k, \tilde{v}_k$  are noted in the main text. This leads to the following expressions

$$\begin{aligned} |u_k|^2 &= \sin^2(k/2) + r_k^2 \cos k + r_k s_k \sin k \cos(\phi_k - \omega_k) \\ |v_k|^2 &= \cos^2(k/2) - r_k^2 \cos k - r_k s_k \sin k \cos(\phi_k - \omega_k) \\ u_k v_k^* &= i \frac{\sin k}{2} (r_k^2 - s_k^2) - i r_k s_k \cos k \cos(\phi_k - \omega_k) - r_k s_k \sin(\phi_k - \omega_k), \end{aligned} \quad (11)$$

where  $r_k = e^{-\pi\tau_Q\Delta^2/2}$ ,  $s_k = \text{sgn}(\Delta)\sqrt{1-r_k^2}$ , and  $\phi_k, \omega_k$  are defined in the main text. Plugging this into Eq. 8, changing the sum to integral as  $(2/N) \sum_{k>0} \rightarrow (1/\pi) \int_0^\pi$  in the limit  $N \rightarrow \infty$ , and further extending the limits of the integral from  $[0, \pi]$  to  $[0, \infty]$  whenever the integrand contains a Gaussian factor of the form  $\sim e^{-\pi\tau_Q k^2}$  (see the definitions of  $r_k, s_k$ ), we obtain the expression of the kink correlator  $\rho(r)$  noted in Eq. 5 in the main text for  $r \gg 1$ . The following identity is used

$$\int_0^\infty dx e^{-bx^2} \cos(ax) = \sqrt{\frac{\pi}{4b}} e^{-a^2/4b}. \quad (12)$$

The behavior of  $\rho(r)$  for fast ramps ending at  $g = 0$  are shown in Fig. 1 (a) and for those extended to  $g = -\infty$ , in (b) and (c) for fast and slow ramps respectively.

## COMPUTATION OF THE KINK CORRELATION FUNCTION IN THE TRANSVERSE DIRECTION

The (connected) kink correlation function in the transverse direction is

$$\begin{aligned}
\chi(r) &= \langle (1 - \sigma_j^z \sigma_{j+1}^z)(1 - \sigma_{j+r}^z \sigma_{j+r+1}^z) \rangle - \langle 1 - \sigma_j^z \sigma_{j+1}^z \rangle \langle 1 - \sigma_{j+r}^z \sigma_{j+r+1}^z \rangle \\
&= \langle \sigma_j^z \sigma_{j+1}^z \sigma_{j+r}^z \sigma_{j+r+1}^z \rangle - \langle \sigma_j^z \sigma_{j+1}^z \rangle \langle \sigma_{j+r}^z \sigma_{j+r+1}^z \rangle \\
&= \langle \mu_j^x \mu_{j+2}^x \mu_{j+r}^x \mu_{j+r+2}^x \rangle - \langle \mu_j^x \mu_{j+2}^x \rangle \langle \mu_{j+r}^x \mu_{j+r+2}^x \rangle,
\end{aligned} \tag{13}$$

where in the last line, the duality relations mentioned in the main text are invoked. Introducing fermionic operators  $A_j = c_j^\dagger + c_j$  and  $B_j = c_j^\dagger - c_j$ , making use of the identity  $\text{Exp}[i\pi c_j^\dagger c_j] = A_j B_j$ , and denoting  $\langle A_j B_{j+r} \rangle \equiv G(r)$ , we find

$$\chi(r) = \begin{vmatrix} G(-1) & G(0) & G(r-1) & G(r) \\ G(-2) & G(-1) & G(r-2) & G(r-1) \\ G(-r-1) & G(-r) & G(-1) & G(0) \\ G(-r-2) & G(-r-1) & G(-2) & G(-1) \end{vmatrix} - \begin{vmatrix} G(-1) & G(0) \\ G(-2) & G(-1) \end{vmatrix}^2, \tag{14}$$

where we have used Wick contraction of a string of operators of the form  $\langle B_j A_{j+1} B_{j+1} A_{j+2} B_{j+r} A_{j+r+1} B_{j+r+1} A_{j+r+2} \rangle$ . Note only terms like  $A_j B_{j+r}$  survive the contraction (terms like  $A_j A_{j+r}$  and  $B_j B_{j+r}$  vanish). It then remains to calculate  $G(r)$  and using the formulation described in the previous section, we obtain

$$\chi(r) \approx -\frac{\zeta}{4\pi^2 \tau_Q} e^{-r^2/2\pi\tau_Q}, \tag{15}$$

where  $\zeta = 1$  for ramps ending at  $g = 0$  and  $\zeta = 1 + (-1)^r$  for ramps ending at  $g = -\infty$ .

### DENSITY MATRIX IN A GGE

Calculations in this section are done following Ref. 2. The formulation applies for a quench from an initial state specified by  $g = g_I$  to a final state specified by  $g = g_F$ . In momentum space, the Hamiltonian  $\tilde{\mathcal{H}}$  reads

$$\mathcal{H} = \sum_k \begin{pmatrix} c_k^\dagger & c_{-k} \end{pmatrix} \begin{pmatrix} 1 - g \cos k & -ig \sin k \\ ig \sin k & g \cos k - 1 \end{pmatrix} \begin{pmatrix} c_k \\ c_{-k}^\dagger \end{pmatrix}. \tag{16}$$

The Bogoliubov-de Gennes transformation  $c_k = u_k \gamma_k + v_{-k}^* \gamma_{-k}^\dagger$  brings it to a diagonal form

$$\mathcal{H} = \sum_k \begin{pmatrix} \gamma_k^\dagger & \gamma_{-k} \end{pmatrix} \begin{pmatrix} \sqrt{1 - 2g \cos k + g^2} & 0 \\ 0 & -\sqrt{1 - 2g \cos k + g^2} \end{pmatrix} \begin{pmatrix} \gamma_k \\ \gamma_{-k}^\dagger \end{pmatrix}. \tag{17}$$

As the Hamiltonian in Eq. 16 is an ensemble of two level systems in  $k$ -space, the initial state (before the quench) can be written as

$$|\Psi_I\rangle = |r_{k_1}, r_{-k_1}\rangle \otimes \cdots \otimes |r_{k_j}, r_{-k_j}\rangle \otimes \cdots \tag{18}$$

This state could be an eigenstate of the Hamiltonian at  $g = g_I$  or one obtained from the ramp stopped at  $g = g_I$ . Time evolution of this state is dictated by the final Hamiltonian  $H_F$  (with  $g = g_F$ ) as

$$|\Psi(t)\rangle = e^{-iH_F t} |\Psi_I\rangle = \sum_n e^{-iE_n t} |n\rangle \langle n | \Psi_I\rangle = \sum_n e^{-iE_n t} |n\rangle c_n, \tag{19}$$

where  $c_n$  is the overlap of the initial state with the  $n$ -th eigenstate of the final Hamiltonian which can also be written as

$$|n\rangle = |p_{k_1}^{[n]}, p_{-k_1}^{[n]}\rangle \otimes \cdots \otimes |p_{k_j}^{[n]}, p_{-k_j}^{[n]}\rangle \otimes \cdots, \tag{20}$$

where  $|p_k^{[n]}, p_{-k}^{[n]}\rangle$  denotes the occupation of Bogoliubov fermions with  $k$  and  $-k$  in the  $n$ -th eigenstate (in a given parity sector) while each  $\{k, -k\}$  subspace is spanned by the four vectors  $\{|0, 0\rangle, |1, 1\rangle, |1, 0\rangle, |0, 1\rangle\}$ . The occupation of the Bogoliubov fermions  $\gamma_k^\dagger \gamma_k$  are conserved quantities (denoted further,  $J_k$ ).



Observables in integrable systems are expected to relax according to a GGE which is defined by the density matrix

$$\varrho_{\text{GGE}} = Z^{-1} e^{-\sum_k \lambda_k J_k}, \quad (21)$$

where  $Z$  is the partition function given by  $Z = \text{Tr}[e^{-\sum_k \lambda_k J_k}]$  and  $J_k$  denotes the conserved quantities. The Lagrange multipliers are fixed by the condition  $\langle \Psi_I | J_k | \Psi_I \rangle \equiv \langle J_k \rangle_I = \text{Tr}[\varrho_{\text{GGE}} J_k]$  which leads to

$$\lambda_k = \ln \left[ \frac{1 - \langle J_k \rangle_I}{\langle J_k \rangle_I} \right]. \quad (22)$$

One can write  $\varrho_{\text{GGE}}$  as a sum over the contribution from all the eigenstates of the Hamiltonian

$$\varrho_{\text{GGE}} = \sum_n \varrho_{\text{GGE}}^{[n]} |n\rangle \langle n|, \quad (23)$$

where

$$\varrho_{\text{GGE}}^{[n]} = \prod_k^{p_k^{[n]}=0} (1 - \langle J_k \rangle_I) \prod_k^{p_k^{[n]}=1} \langle J_k \rangle_I, \quad (24)$$

using  $\langle n | e^{-\lambda_k J_k} | n \rangle = \delta_{p_k^{[n]}, 0} + e^{-\lambda_k} \delta_{p_k^{[n]}, 1}$  (both  $k$  and  $-k$  are included in the above product). To complete the discussion, what remains is to compute  $\langle J_k \rangle_I$ .

Calculating  $\langle J_k \rangle_I$  involves the overlap  $c_n$  in Eq. 19 which is the product of the overlaps (for a chain of length  $N$ , it is a product over  $N/2$  terms in each of the parity sectors) in each subspace  $\{k, -k\}$  as  $c_n = \prod_k c_k^{[n]}$ . Denoting the initial state as a tensor product  $|\Psi_I\rangle = \otimes_k [u_k^{(I)} \ v_k^{(I)}]^T$  and that corresponding to the final state  $|\Psi_F\rangle = \otimes_k [u_k^{(F)} \ v_k^{(F)}]^T$ , we have

$$c_k^{[n]} = \begin{cases} \pm \sqrt{\alpha_k} & \equiv c_k^{(1)}, & \text{if } p_k^{[n]} = r_k \text{ and } p_{-k}^{[n]} = r_{-k}, \\ 0 & \equiv c_k^{(2)}, & \text{if } p_k^{[n]} = 1 \text{ and } p_{-k}^{[n]} = 0, \\ 0 & \equiv c_k^{(3)}, & \text{if } p_k^{[n]} = 0 \text{ and } p_{-k}^{[n]} = 1, \\ \pm i \sqrt{1 - \alpha_k} & \equiv c_k^{(4)}, & \text{if } p_k^{[n]} \neq r_k \text{ and } p_{-k}^{[n]} \neq r_{-k}, \end{cases} \quad (25)$$

for  $r_k = r_{-k} = 0$  and  $r_k = r_{-k} = 1$ , and

$$c_k^{[n]} = \begin{cases} 0 \equiv c_k^{(1)}, & \text{if } p_k^{[n]} = 0 \text{ and } p_{-k}^{[n]} = 0, \\ 1 \equiv c_k^{(2)}, & \text{if } p_k^{[n]} = r_k \text{ and } p_{-k}^{[n]} = r_{-k}, \\ 0 \equiv c_k^{(3)}, & \text{if } p_k^{[n]} \neq r_k \text{ and } p_{-k}^{[n]} \neq r_{-k}, \\ 0 \equiv c_k^{(4)}, & \text{if } p_k^{[n]} = 1 \text{ and } p_{-k}^{[n]} = 1, \end{cases} \quad (26)$$

for  $r_k = 0$  and  $r_{-k} = 1$ , or,  $r_k = 1$  and  $r_{-k} = 0$ . Note  $\sum_\xi |c_k^{(\xi)}|^2 = 1$  is implied by the normalization of the initial state  $\langle \Psi_I | \Psi_I \rangle = 1$ .

Using the notation in Eq. 25 and Eq. 26 we find  $\langle J_k \rangle_I = |c_k^{(\xi)}|^2$  with  $p_k^{[n]} = 1$  while  $\xi$  is determined by  $\{r_k, r_{-k}\}$  and so

$$\langle J_k \rangle_I = \begin{cases} 1 - \alpha_k, & \text{if } r_k = 0 \text{ and } r_{-k} = 0, \\ \alpha_k, & \text{if } r_k = 1 \text{ and } r_{-k} = 1, \\ 0, & \text{if } r_k = 1 \text{ and } r_{-k} = 0, \\ 0, & \text{if } r_k = 0 \text{ and } r_{-k} = 1, \end{cases} \quad (27)$$

where

$$\alpha_k = |u_k^{(I)*} u_k^{(F)} + v_k^{(I)*} v_k^{(F)}|^2. \quad (28)$$

As the initial state prepared at the end of the ramp obeys  $\gamma_k \gamma_{-k} |\Psi_I\rangle = 0$ , it corresponds to  $r_k = r_{-k} = 0$  in Eq. 18 implying  $\langle J_k \rangle_I = 1 - \alpha_k$  and

$$\varrho_{\text{GGE}}^{[n]} = \prod_k^{p_k^{[n]}=0} \alpha_k^2 \prod_k^{p_k^{[n]} \neq p_{-k}^{[n]}} \alpha_k (1 - \alpha_k) \prod_k^{p_k^{[n]}=1} (1 - \alpha_k)^2. \quad (29)$$

### KINK CORRELATION IN A GGE

As noted in the main text, the (longitudinal) kink correlator is

$$\hat{\rho}(r) = \mu_j^z \mu_{j+r}^z - \langle \mu_j^z \rangle^2. \quad (30)$$

Introducing fermionic operators  $A_j = c_j^\dagger + c_j$  and  $B_j = c_j^\dagger - c_j$ , we can write  $\mu_j^z \equiv 1 - 2c_j^\dagger c_j = A_j B_j$ . Further denoting  $A_j B_{j+r} \equiv \hat{G}(r)$ , we find

$$\langle \hat{\rho}(r) \rangle_{\text{GGE}} = - \sum_n \varrho_{\text{GGE}}^{[n]} \langle n | \hat{G}(r) | n \rangle \langle n | \hat{G}(-r) | n \rangle, \quad (31)$$

where  $\langle n | \hat{G}(r) | n \rangle$ , written in terms of the occupation of the Bogoliubov fermions, is

$$\langle n | \hat{G}(r) | n \rangle = \frac{2}{N} \sum_{k>0} (p_k^{[n]} + p_{-k}^{[n]} - 1) \mathcal{G}, \quad (32)$$

with

$$\mathcal{G} = \frac{g \sin k \sin(kr)}{\sqrt{1 - 2g \cos k + g^2}} - \frac{(1 - g \cos k) \cos(kr)}{\sqrt{1 - 2g \cos k + g^2}}. \quad (33)$$

Expectation value of an operator  $\hat{\mathcal{A}}$  in the GGE with weights  $\{\varrho_{\text{GGE}}^{[n]}\}$  is given by

$$\langle \hat{\mathcal{A}} \rangle_{\text{GGE}} = \sum_n \varrho_{\text{GGE}}^{[n]} \langle n | \hat{\mathcal{A}} | n \rangle. \quad (34)$$

Provided  $\langle n | \hat{\mathcal{A}} | n \rangle$  is a sum of single particle contribution as  $\langle n | \hat{\mathcal{A}} | n \rangle = \sum_k \langle n | \hat{\mathcal{A}}_k | n \rangle$  and the weight  $\varrho_{\text{GGE}}^{[n]}$  factorizes as  $\varrho_{\text{GGE}}^{[n]} = \prod_k \varrho_{k, \text{GGE}}^{[n]}$ , Eq. 34 can be rewritten as

$$\langle \hat{\mathcal{A}} \rangle_{\text{GGE}} = \sum_{k>0} \left( \sum_{\xi} \varrho_{k, \text{GGE}}^{(\xi)} \hat{\mathcal{A}}_k^{(\xi)} \right), \quad (35)$$

where we have introduced the notation

$$\varrho_{k, \text{GGE}}^{[n]} = \begin{cases} \varrho_{k, \text{GGE}}^{(1)}, & \text{if } p_k^{[n]} = 0 \text{ and } p_{-k}^{[n]} = 0, \\ \varrho_{k, \text{GGE}}^{(2)}, & \text{if } p_k^{[n]} = 1 \text{ and } p_{-k}^{[n]} = 0, \\ \varrho_{k, \text{GGE}}^{(3)}, & \text{if } p_k^{[n]} = 0 \text{ and } p_{-k}^{[n]} = 1, \\ \varrho_{k, \text{GGE}}^{(4)}, & \text{if } p_k^{[n]} = 1 \text{ and } p_{-k}^{[n]} = 1, \end{cases} \quad (36)$$

and

$$\langle n | \hat{\mathcal{A}}_k | n \rangle = \begin{cases} \hat{\mathcal{A}}_k^{(1)}, & \text{if } p_k^{[n]} = 0 \text{ and } p_{-k}^{[n]} = 0, \\ \hat{\mathcal{A}}_k^{(2)}, & \text{if } p_k^{[n]} = 1 \text{ and } p_{-k}^{[n]} = 0, \\ \hat{\mathcal{A}}_k^{(3)}, & \text{if } p_k^{[n]} = 0 \text{ and } p_{-k}^{[n]} = 1, \\ \hat{\mathcal{A}}_k^{(4)}, & \text{if } p_k^{[n]} = 1 \text{ and } p_{-k}^{[n]} = 1. \end{cases} \quad (37)$$

Similarly, it is straightforward to show the identity

$$\begin{aligned} \sum_n \varrho_{k, \text{GGE}}^{[n]} \langle n | \hat{\mathcal{A}}_1 | n \rangle \langle n | \hat{\mathcal{A}}_2 | n \rangle &= \langle \hat{\mathcal{A}}_1 \rangle_{\text{GGE}} \langle \hat{\mathcal{A}}_2 \rangle_{\text{GGE}} - \sum_{k>0} \left( \sum_{\xi} \varrho_{k, \text{GGE}}^{(\xi)} \hat{\mathcal{A}}_{1,k}^{(\xi)} \right) \left( \sum_{\xi'} \varrho_{k, \text{GGE}}^{(\xi')} \hat{\mathcal{A}}_{2,k}^{(\xi')} \right) \\ &+ \sum_{k>0} \left( \sum_{\xi} \varrho_{k, \text{GGE}}^{(\xi)} \hat{\mathcal{A}}_{1,k}^{(\xi)} \hat{\mathcal{A}}_{2,k}^{(\xi)} \right), \end{aligned} \quad (38)$$

where  $\langle \hat{\mathcal{A}}_{1/2} \rangle_{\text{GGE}}$  is defined according to Eq. 35 and  $\hat{\mathcal{A}}_{1/2,k}^{(\xi)}$  is defined according to Eq. 37. Using Eq. 29 to Eq. 38, we obtain

$$\langle \hat{\rho}(r) \rangle_{\text{GGE}} = -\langle \hat{G}(r) \rangle_{\text{GGE}} \langle \hat{G}(-r) \rangle_{\text{GGE}} + \frac{4}{N^2} \sum_{k>0} 2\alpha_k (1 - \alpha_k) \sin^2(kr), \quad (39)$$

where

$$\langle \hat{G}(r) \rangle_{\text{GGE}} = \frac{2}{N} \sum_{k>0} (2\alpha_k - 1) \mathcal{G}. \quad (40)$$

Note the last term in Eq. 39 vanishes in the thermodynamic limit.

Let us denote the wavefunction at  $k$  obtained immediately after stopping the ramp at  $g = 0$  as the initial state  $[u_k^{(I)}, v_k^{(I)}]^T$  and that obtained by diagonalizing  $\mathcal{H}$  at  $k$  for  $g = 0$  as the final state  $[u_k^{(F)}, v_k^{(F)}]^T$ . Then the overlap function  $\alpha_k$  defined in Eq. 28 takes the form

$$\alpha_k \approx |u_k^{(I)}|^2 |u_k^{(F)}|^2 + |v_k^{(I)}|^2 |u_k^{(F)}|^2, \quad (41)$$

where we have neglected the cross terms that contain the rapidly oscillating phases  $e^{i\omega_k}$  and  $e^{i\phi_k}$  (defined in the main text) for  $\tau_Q \gg 1$  and, hence, vanish in the sum over  $k$ . The results are plotted in Fig. 2 of the main text. Note that for an instantaneous quench, the correlation function resembles those of the eigenstates of the initial Hamiltonian, which decay exponentially [see Fig. 2 (a)].

### KINK CORRELATION FUNCTION AT LATE TIMES

Let us assume we have stopped the ramp at  $g = g_0$  that yields the wavefunction  $[u_k^{(I)}, v_k^{(I)}]^T$  which then evolves to  $[u_k(t), v_k(t)]^T$  under the static Hamiltonian (Eq. 1 in the main text) at  $g = g_0$ . The dynamics is governed by the Schrödinger equation

$$i\partial_t \begin{pmatrix} u_k \\ v_k \end{pmatrix} = \begin{pmatrix} g_0 - \cos k & -i \sin k \\ i \sin k & \cos k - g_0 \end{pmatrix} \begin{pmatrix} u_k \\ v_k \end{pmatrix} \equiv H_k \begin{pmatrix} u_k \\ v_k \end{pmatrix}, \quad (42)$$

where time dependence in  $u_k, v_k$  is implied. If the unitary matrix  $U_k$  diagonalizes  $H_k$  such that  $U_k^\dagger H_k U_k = \Sigma_k$  where  $\Sigma_k = \varepsilon_k \begin{pmatrix} -1 & 0 \\ 0 & 1 \end{pmatrix}$  with  $\varepsilon_k = \sqrt{1 - 2g_0 \cos k + g_0^2}$ , then the diagonal modes  $\tilde{u}_k, \tilde{v}_k$  satisfy

$$i\partial_t \begin{pmatrix} \tilde{u}_k \\ \tilde{v}_k \end{pmatrix} = \begin{pmatrix} -\varepsilon_k & 0 \\ 0 & \varepsilon_k \end{pmatrix} \begin{pmatrix} \tilde{u}_k \\ \tilde{v}_k \end{pmatrix}. \quad (43)$$

These diagonal modes are connected with the original modes as

$$\begin{pmatrix} \tilde{u}_k \\ \tilde{v}_k \end{pmatrix} = U_k^\dagger \begin{pmatrix} u_k \\ v_k \end{pmatrix} = \begin{pmatrix} -\sin(\theta_k/2) & -i \cos(\theta_k/2) \\ \cos(\theta_k/2) & -i \sin(\theta_k/2) \end{pmatrix} \begin{pmatrix} u_k \\ v_k \end{pmatrix}, \quad (44)$$

where  $\cos \theta_k = (g_0 - \cos k)/\varepsilon_k$ . If  $\tilde{u}_k, \tilde{v}_k$  are specified by their initial values  $\tilde{u}_k^{(I)}, \tilde{v}_k^{(I)}$ , then their values at time  $t$  (assuming the ramp stopped at  $t = 0$  when the subsequent evolution starts) is

$$\tilde{u}_k(t) = e^{i\varepsilon_k t} \tilde{u}_k^{(I)} \quad ; \quad \tilde{v}_k(t) = e^{-i\varepsilon_k t} \tilde{v}_k^{(I)}. \quad (45)$$

Noting  $[\tilde{u}_k^{(I)}, \tilde{v}_k^{(I)}]^T = U_k^\dagger [u_k^{(I)}, v_k^{(I)}]^T$ , we obtain the solution  $u_k, v_k$  as

$$\begin{pmatrix} u_k \\ v_k \end{pmatrix} = U_k e^{-i\Sigma_k t} U_k^\dagger \begin{pmatrix} u_k^{(I)} \\ v_k^{(I)} \end{pmatrix}. \quad (46)$$

Written out explicitly and ignoring all the rapidly oscillating terms as done before leads to, at late times,

$$|u_k|^2 \approx \frac{1}{2} (1 + \cos^2 \theta_k) |u_k^{(I)}|^2 + \frac{1}{2} (1 - \cos^2 \theta_k) |v_k^{(I)}|^2 \quad ; \quad |v_k|^2 = 1 - |u_k|^2 \quad ; \quad u_k v_k^* = \frac{i}{2} \sin \theta_k \cos \theta_k \left( |v_k^{(I)}|^2 - |u_k^{(I)}|^2 \right). \quad (47)$$

We plug these expressions in Eq. 8 to obtain the plot shown in Fig. 2 of the main text. The results perfectly match with that obtained from the GGE computed in the previous section, as also displayed in Fig. 2 of the main text.

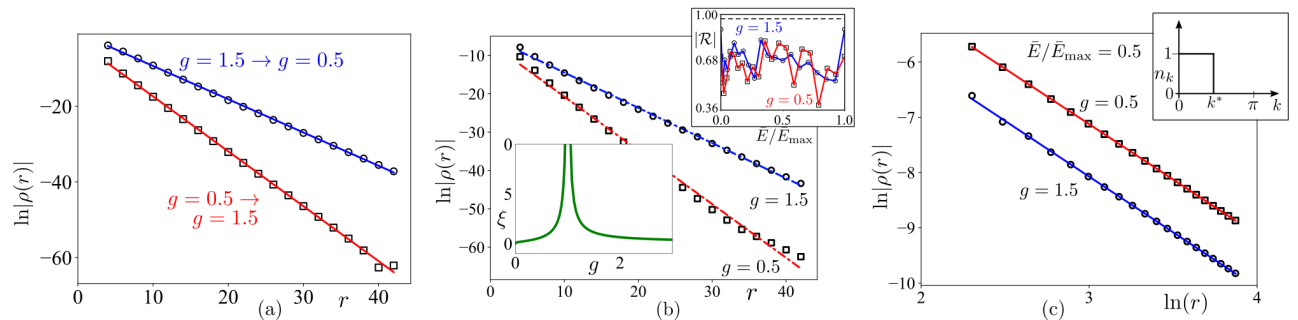


FIG. 2. (a) A plot of  $\ln|\rho(r)|$  vs  $r$  calculated from the GGE density matrix  $\rho_{\text{GGE}}$  (defined in the text) for instantaneous quenches that reflects the ground state behavior shown in (b) consistent with KZM. The symbols stand for the numerical data and the lines, the best fit. (b) Kink correlation in the eigenstates: Exponential decay of the kink correlation function in the paramagnetic ( $g = 1.5$ ) and in the ferromagnetic ( $g = 0.5$ ) phase for the ground state of the static Hamiltonian  $\mathcal{H}$  in Eq. 1 in the main text with  $J = 1$  (the symbols stand for the numerical data and the lines, the best fit). Inset top right: Behavior of  $|\mathcal{R}|$  (defined in the text) for eigenstates of  $\mathcal{H}$  specified by their normalized energy density  $\bar{E}/\bar{E}_{\text{max}}$  (defined in the main text) which clearly indicates absence of Gaussian behavior of the kink-kink correlator in any of these box eigenstates (defined in the text). The bottom left inset shows the behavior of the correlation length  $\xi$  (defined in the text) as a function of the field  $g$  which diverges at the critical point  $g = 1$ . (c) Kink correlation for a box eigenstate at energy density  $\bar{E}/\bar{E}_{\text{max}} = 0.5$  that shows an algebraic decay:  $\rho(r) \sim r^{-2}$ . The empty circles correspond to the paramagnetic phase ( $g = 1.5$ ) and the empty squares represent the ferromagnetic phase ( $g = 0.5$ ). The blue and red dashed lines represent the best fit for  $g = 1.5$  and  $g = 0.5$  respectively. The inset shows the profile of occupation probability  $n_k$  used to generate a box eigenstate as a function of  $k$  with  $k$ -modes up to  $k = k^*$  excited.

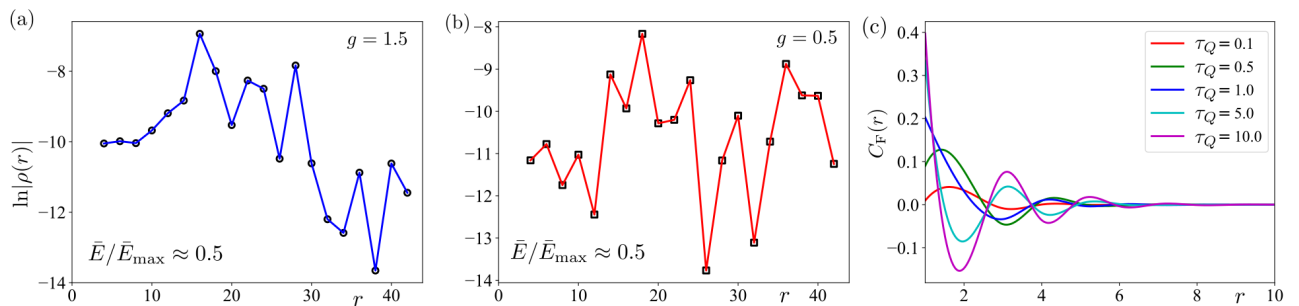


FIG. 3. Kink correlation in a random eigenstate generated by exciting a randomly selected set of  $k$ -modes in the (a) paramagnetic phase ( $g = 1.5$ ) and (b) ferromagnetic phase ( $g = 0.5$ ) with concomitant energy density  $\bar{E}/\bar{E}_{\text{max}} \approx 0.5$ . (c) Fermion correlation  $C_F(r)$  (defined in the text) for rapid ramps at different (small) values of  $\tau_Q$  showing oscillating (decaying) exponential.

### KINK CORRELATION FUNCTION IN THE EIGENSTATES OF THE STATIC MODEL

For the static model, let us calculate the kink correlation in the ground state  $|n_G\rangle = |0, 0\rangle \otimes \cdots \otimes |0, 0\rangle$  of  $\tilde{\mathcal{H}}$  (defined in the main text) which is in fact the same measured in the highest excited state  $|n_E\rangle = |1, 1\rangle \otimes \cdots \otimes |1, 1\rangle$  of  $\tilde{\mathcal{H}}$  or equivalently the ground state of  $\mathcal{H}$  (Eq. 1 of the main text). The correlation function is given by

$$\langle \hat{\rho}(r) \rangle_\mu = -\langle n_\mu | \hat{G}(r) | n_\mu \rangle \langle n_\mu | \hat{G}(-r) | n_\mu \rangle, \quad (48)$$

where  $\mu = G, E$ . For the ground state and the highest excited state,

$$\langle n_E | \hat{G}(r) | n_E \rangle = -\langle n_G | \hat{G}(r) | n_G \rangle = \frac{2}{N} \sum_{k>0} \mathcal{G} = \frac{1}{\pi} \int_0^\pi dk \mathcal{G} \equiv -\mathcal{I}(r), \quad (49)$$

( $\mathcal{G}$  defined in Eq. 33) implying  $\langle \hat{\rho}(r) \rangle_G = \langle \hat{\rho}(r) \rangle_E$ .

Let us now analyze the asymptotes of  $\mathcal{I}(r)$  for large  $r$ . A straightforward integration using Mathematica yields

$$\mathcal{I}(r) = \frac{\pi}{|1+g|} \left[ {}_3F_2(1/2, 1/2, 1; 1-r, 1+r; z) - g {}_3F_2(1/2, 1/2, 1; 2-r, r; z) \right] \equiv \pi \frac{\mathcal{A} - g\mathcal{B}}{|1+g|}, \quad (50)$$

where  $z = 4g/(1+g)^2$  ( $0 \leq |z| \leq 1$ ). The quantity  ${}_p\mathcal{F}_q$  denotes the *regularized generalized Hypergeometric function* of the form

$${}_p\mathcal{F}_q(a_1, \dots, a_p; b_1, \dots, b_q; z) = \sum_{k=0}^{\infty} T(k) z^k; \quad T(k) = \frac{1}{k!} \frac{(a_1)_k \dots (a_p)_k}{(b_1)_k \dots (b_q)_k} \frac{1}{\Gamma(b_1) \dots \Gamma(b_q)}, \quad (51)$$

where  $(a_l)_k$  [or  $(b_l)_k$ ] is called the rising factorial or *Pochhammer symbol* defined as  $(a_l)_k = \Gamma(a_l + k)/\Gamma(a_l)$ . Since the hypergeometric series is unimodal, the ratio of two consecutive terms in, e.g.,  $\mathcal{A}$  in Eq. 50, which has the form

$$\begin{aligned} R_{\mathcal{A}} &= \frac{T(k+1)z^{k+1}}{T(k)z^k} = \left(\frac{z}{k+1}\right) \left(\frac{\Gamma^2(k+3/2)\Gamma(k+2)}{\Gamma^2(k+1/2)\Gamma(k+1)}\right) \left(\frac{\Gamma(k+1-r)\Gamma(k+1+r)}{\Gamma(k+2-r)\Gamma(k+2+r)}\right) \\ &= \left(\frac{z}{k+1}\right) \left(\frac{(k+1/2)^2(k+1)}{(k+1-r)(k+1+r)}\right) \end{aligned} \quad (52)$$

(using the recurrence relation of the Gamma functions  $\Gamma(z+1) = z\Gamma(z)$  in the last line), should be equal to 1 for  $k = k_{\max} \equiv k_0$ . At large values of  $r$ , we find  $k_0 \approx r/\sqrt{1-z}$  which also holds for  $\mathcal{B}$ . Exploiting its unimodular nature, the series  $\mathcal{A}$  can be approximated by an integral of the form

$$\mathcal{A} \approx \int_{-\infty}^{\infty} dk e^{k \ln(z) + f(k)} \approx \int_{-\infty}^{\infty} dk e^{k_0 \ln(z) + f(k_0) + (k-k_0)^2 f''(k_0)/2}, \quad (53)$$

where we have Taylor expanded the function  $f(k) \equiv \ln[T(k)]$  around  $k = k_0$  retaining terms up to quadratic order and using the fact  $f'(k_0) = 0$ . Noting

$$f(k) \approx \ln \left[ \frac{1}{k!} \frac{\Gamma^3(k)}{\Gamma(k+r)\Gamma(k-r)} \right], \quad (54)$$

and invoking Stirling's approximation of the logarithm of Gamma function and logarithm of factorial, and following the same procedure for  $\mathcal{B}$ , we finally obtain

$$\mathcal{I}(r) \sim e^{-r/\xi}; \quad \xi^{-1} = |\ln(4g) - 2\ln(1+g)| + 2\sqrt{(1-g)^2/(1+g)^2}, \quad (55)$$

Note the correlation length  $\xi$  diverges at  $g = 1$  as expected [Fig. 2 (b) bottom left inset] and the same expression holds for  $\mathcal{I}(-r)$  as well. The exponentially falling nature of  $\rho(r)$  in different phases is shown in Fig. 2 (b).

Finally, let us calculate  $\rho(r)$  in a mixed state  $|n_M\rangle = |1, 1\rangle \otimes \dots \otimes |1, 1\rangle \otimes |0, 0\rangle|0, 0\rangle$  where a tensor product of the excited states  $|1, 1\rangle$  is considered up to  $k = k^*$ , and a tensor product of the ground states  $|0, 0\rangle$  is considered for the rest of the  $k$ -values. We call this state a ‘‘box eigenstate’’ because of the profile of occupation probability  $n_k$  shown in the inset of Fig. 2 (c). In this state, we have

$$\langle n_M | \hat{G}(r) | n_M \rangle = -\frac{1}{\pi} \int_{k^*}^{\pi} dk \mathcal{G} + \frac{1}{\pi} \int_0^{k^*} dk \mathcal{G}, \quad (56)$$

while the associated energy density is  $\bar{E} = (2/\pi) \int_0^{k^*} dk \sqrt{1 - 2g \cos k + g^2}$  [further normalized with respect to the maximum energy density  $\bar{E}_{\max} = \bar{E}(k^* = \pi)$ ]. Fig. 2 (c) displays the behavior of  $\rho(r)$  in a typical box eigenstate at  $\bar{E}/\bar{E}_{\max} = 0.5$  which shows an asymptotic algebraic decay:  $\rho(r) \sim r^{-2}$  as obtained from integration by parts of the integrands in Eq. 56. A plot of the absolute value of Pearson coefficient  $|\mathcal{R}|$  (defined in the last section) as a function of  $\bar{E}/\bar{E}_{\max}$  is plotted in the inset of Fig. 2 (b) implying absence of Gaussian in the kink correlation measured in these states.

We also generate a family of random eigenstates  $|n_R\rangle$  by exciting a random set of  $k$ -modes with a given probability and measure the kink correlation in those states. Again we find no trace of Gaussian in any of such states [see Fig. 3 (a)-(b)] establishing the fact that no eigenstate of  $\mathcal{H}$  can feature the Gaussian behavior, and hence, what we are observing for the ramp is truly a dynamical effect.

## SPIN CORRELATION

Following Ref. 3, the spin correlation or equivalently the (nonlocal) fermionic correlation function is

$$\begin{aligned} C_F(r) &= \langle \sigma_j^x \sigma_{j+r}^x \rangle = \langle B_j (A_{j+1} B_{j+1} \dots A_{j+r-1} B_{j+r-1}) A_{j+r} \rangle \\ &= \begin{vmatrix} G(-1) & G(-2) & \dots & G(-r) \\ G(0) & G(-1) & \dots & G(-r+1) \\ \dots & \dots & \dots & \dots \\ G(r-2) & G(r-3) & \dots & G(-1) \end{vmatrix}, \end{aligned} \quad (57)$$

where  $G(r) \equiv \langle A_j B_{j+r} \rangle = (1/\pi) \int_0^\pi dk (|u_k|^2 - |v_k|^2) \cos(kr)$  is the relevant two-point fermionic correlator [4]. Fig. 3 (c) shows the behavior of  $C_F(r)$  against  $r$  for rapid ramps at various (small) values of  $\tau_Q$  which features oscillations with an exponentially decaying envelope. Furthermore, approximating the quantity  $(|v_k|^2 - |u_k|^2) = 1 - 2r_k^2$  by a thermal occupancy of the form  $(1 + e^{\varepsilon_k/T})^{-1}$  leads to the expressions of  $\varepsilon_k$  and  $T^*$  noted in the main text.

### PEARSON CORRELATION COEFFICIENT

For a paired dataset  $\mathcal{D} := \{(x_i, y_i)\}$ , the correlation coefficient  $\mathcal{R} (\in [-1, 1])$  of the best fit is given by [5]

$$\mathcal{R} = (\langle XY \rangle - \langle X \rangle \langle Y \rangle) / (\sigma_X \sigma_Y), \quad (58)$$

where  $\langle X(Y) \rangle$  denotes the mean of the sample set  $X = \{x_i\}$  ( $Y = \{y_i\}$ ) and  $\sigma$ , the standard deviation. If  $|\mathcal{R}| = 1$ , the data is said to have a perfect linear correlation (all points are on the best fit) while  $|\mathcal{R}| = 0$  implies no correlation whatsoever. Accordingly, if the data is perfectly Gaussian correlated,  $|\mathcal{R}|$  is 1 for  $X = \{x_i^2\}$  and  $Y = \{\ln|y_i|\}$  and deviation from  $|\mathcal{R}| = 1$  suggests departure from Gaussian. Following this, we compute  $|\mathcal{R}|$  for our numerical data  $\mathcal{D} := \{(\tau_i^2, \ln|\rho_i|)\}$  and study its behavior as a function of  $\hat{g}$  for different values of  $\tau_Q$  as reported in the main text. This is also used in verifying the absence of Gaussian in the box eigenstates of the Hamiltonian as shown in Fig. 2 (b).

- 
- [1] E. T. Whittaker and G. N. Watson. *A Course in Modern Analysis (4th Ed.)*. Cambridge University Press, 1990.
  - [2] Lev Vidmar and Marcos Rigol. Generalized gibbs ensemble in integrable lattice models. *Journal of Statistical Mechanics: Theory and Experiment*, 2016(6):064007, 2016.
  - [3] Sei Suzuki, Jun-ichi Inoue, and Bikas K Chakrabarti. *Quantum Ising phases and transitions in transverse Ising models*, volume 862. Springer, 2012.
  - [4] R. W. Cherng and L. S. Levitov. Entropy and correlation functions of a driven quantum spin chain. *Phys. Rev. A*, 73:043614, Apr 2006.
  - [5] Karl Pearson. Vii. note on regression and inheritance in the case of two parents. *proceedings of the royal society of London*, 58(347-352):240–242, 1895.